1521-009X/41/5/1060–1069$25.00
DRUG METABOLISM AND DISPOSITION
http://dx.doi.org/10.1124/dmd.112.050401
Drug Metab Dispos 41:1060–1069, May 2013

Induction of Xenobiotic Receptors, Transporters, and Drug Metabolizing Enzymes by Oxycodone[S]

Hazem E. Hassan, Alan L. Myers,[1] Insong J. Lee,[2] Clifford W. Mason,[3] Duan Wang, Michael W. Sinz, Hongbing Wang, and Natalie D. Eddington

Department of Pharmaceutical Sciences, School of Pharmacy, University of Maryland, Baltimore, Maryland (H.E.H., A.L.M., I.J.L., C.W.M., D.W., H.W., N.D.E.); Bristol-Myers Squibb Co., Wallingford, Connecticut (M.W.S.); and Department of Pharmaceutics and Industrial Pharmacy, Faculty of Pharmacy, Helwan University, Cairo, Egypt (H.E.H.)

Received December 18, 2012; accepted February 25, 2013

ABSTRACT

Perturbations of the expression of transporters and drug-metabolizing enzymes (DMEs) by opioids can be the locus of deleterious drug-drug interactions (DDIs). Many transporters and DMEs are regulated by xenobiotic receptors [XRs; e.g., pregnane X receptor (PXR), constitutive androstane receptor (CAR), and Aryl hydrocarbon receptor (AhR)]; however, there is a paucity of information regarding the influence of opioids on XRs. The objective of this study was to determine the influence of oxycodone administration (15 mg/kg intraperitoneally twice daily for 8 days) on liver expression of XRs, transporters, and DMEs in rats. Microarray, quantitative real-time polymerase chain reaction and immunoblotting analyses were used to identify significantly regulated genes. Three XRs (e.g., PXR, CAR, and AhR), 27 transporters (e.g., ABCB1 and SLC22A8), and 19 DMEs (e.g., CYP2B2 and CYP3A1) were regulated ($P < 0.05$) with fold changes ranging from −46.3 to 17.1. Using MetaCore (computational platform), we identified a unique gene-network of transporters and DMEs assembled around PXR, CAR, and AhR. Therefore, a series of transactivation/translocation assays were conducted to determine whether the observed changes of transporters/DMEs are mediated by direct activation of PXR, CAR, or AhR by oxycodone or its major metabolites (noroxycodone and oxymorphone). Neither oxycodone nor its metabolites activated PXR, CAR, or AhR. Taken together, these findings identify a signature hepatic gene-network associated with repeated oxycodone administration in rats and demonstrate that oxycodone alters the expression of many transporters and DMEs (without direct activation of PXR, CAR, and AhR), which could lead to undesirable DDIs after coadministration of substrates of these transporters/DMEs with oxycodone.

Introduction

Inter-individual variability in the expression patterns of genes encoding for transporters and/or drug-metabolizing enzymes (DMEs) could lead to subtherapeutic or toxic drug levels. As a result, extensive studies have been directed toward elucidating the mechanisms that govern the expression of these genes. One of the major mechanisms involved in the regulation of these genes is transcriptional regulation by xenobiotic receptors [XRs; e.g., pregnane X receptor (PXR), constitutive androstane receptor (CAR), and Aryl hydrocarbon receptor (AhR)] (Kim, 2002; Tirona and Kim, 2005). For example, ABCB1, CYP3A1 (CYP3A4), and CYB2b2 (CYP2B6) are regulated by PXR. CYP3A1 (CYP3A4) and CYB2B2 (CYP2B6) are regulated by CAR, and glutathione S-transferase α and UDP glucuronosyltransferase UGT1A are regulated by AhR (Tirona and Kim, 2005). As such, PXR, CAR, and AhR are promiscuous XRs that translate chemical activation into coordinated induction of transporters and DMEs. The expression of XRs, DMEs, and transporters is prominent in liver, where pharmacokinetic-based drug-drug interactions (DDIs) occur. Coadministration of XR-activators with transporters/DME-substrates can lead to undesirable DDIs. For example, coadministration of rifampin (PXR-activator) with oxycodone (CYP3A4 and ABCB1 substrate) caused a significant reduction in oxycodone plasma concentrations in humans (Nieminen et al., 2009).

Opioids have been extensively used for decades for the management of pain; nonetheless, few studies have examined their ability to regulate the expression of XRs, transporters, and/or DMEs. We have previously reported that methadone activates both PXR and CAR in human primary hepatocytes, which led to the induction of ABCB1, CYP3A4, CYP2B6, and UGT 1A1 (Tolson et al., 2009), while buprenorphine and diprenorphine activate PXR and CAR in HepG2 cells, resulting in CYP3A4 and CYP2B6 induction (Li et al., 2010). Morphine induced the efflux transporter, ABCB1, in rat brain (Aquilante et al., 2000), and oxycodone regulated many transporters (e.g., ABCB1 and ABCG2) and DMEs (e.g., rat glutathione S-transferase α5) in various rat tissues (Hassan et al., 2007, 2010; Myers et al., 2010). Changes in the expression

This study was supported in part by University of Maryland Intramural Research grant (to N.D.E.).

[1]Current affiliation: The University of Texas, MD Anderson Cancer Center, Houston, Texas.

[2]Current affiliation: Department of Pharmaceutical Sciences, Notre Dame of Maryland University, School of Pharmacy, Baltimore, Maryland.

[3]Current affiliation: Department of Obstetrics and Gynecology, University of Kansas School of Medicine, Kansas City, Kansas.

dx.doi.org/10.1124/dmd.112.050401.

[S]This article has supplemental material available at dmd.aspetjournals.org.

ABBREVIATIONS: AhR, Aryl hydrocarbon receptor; CAR, constitutive androstane receptor; CITCO, 6-(4-chlorophenyl)imidazo[2,1-b][1,3]thiazole-5-carbaldehyde *O*-(3,4-dichlorobenzyl oxime; Ct, threshold cycle; DDI, drug-drug interaction; DME, drug-metabolizing enzyme; DMSO, dimethylsulfoxide; FMO, flavin containing monooxygenase; MDR, multidrug resistance proteins; POR, cytochrome P450 oxidoreductase; PXR, pregnane X receptor; qRT-PCR, quantitative real-time polymerase chain reaction; SLC, solute linked carrier; XR, xenobiotic receptor.

of transporters/DMEs by opioids can be the locus of pharmacokinetic– and pharmacodynamic– based DDIs. For example, we demonstrated that oxycodone induced Abcb1 in brain, kidney, liver, and intestine, which hindered paclitaxel (ABCB1 substrate) accumulation in these tissues (Hassan et al., 2007). In addition, we reported that the efflux transporter, ABCG2, was significantly upregulated in brain tissue of oxycodone-treated rats (Hassan et al., 2010), restricting the uptake of mitoxantrone, an ABCG2 substrate.

Nonetheless, the characterization of the complete spectrum of XRs, transporters, and DMEs affected after repeated administration of opioids has not been elucidated in rodents or humans. We hypothesize that repeated opioid administration affects the hepatic expression of XRs, transporters, and DMEs, which can lead to deleterious DDIs. The significance of identifying changes in the expression of these disposition-controlling genes comes from the fact that polypharmacy is a serious clinical concern today, and opioids are commonly coadministered with therapeutic agents (e.g., efavirenz and paclitaxel) or illicit drugs (e.g., cocaine) that are substrates/inhibitors of these genes. As such, identifying these expression changes is crucial for adjusting therapeutic doses and avoiding DDIs. To test our hypothesis, we investigated the influence of repeated oxycodone (representative opioid agonist) administration on the hepatic expression of XRs, transporters, and DMEs in rats. Oxycodone is the opioid of choice for management of pain in the United States (Hays, 2004). The severity of oxycodone use/misuse was well documented by the Drug Abuse Warning Network, which reported a total of 1014 oxycodone-related deaths in a 3-year period (Cone et al., 2003). Ninety percent of these oxycodone-related deaths were attributed to DDIs that can be transporters/DME mediated (Burrows et al., 2003; Cone et al., 2003, 2004; Lee et al., 2006; Nakazawa et al., 2010; Nieminen et al., 2010). We used microarrays to obtain a global profile of genes (including XRs, transporters, and DMEs) regulated in liver tissue of oxycodone treated rats. Then, we validated the changes in expression of many genes by quantitative real-time polymerase chain reaction (qRT-PCR) and immunoblotting analysis. All regulated genes were imported into MetaCore (Thomson Reuters, New York, NY), a Web-based computational platform, to build a highly interconnected gene network of XRs, transporters, and DMEs in the context of rat regulatory interactions reported in the literature. Finally, a series of cell-based XR reporter and translocation assays were conducted to determine the magnitude of differential activation of XRs by oxycodone and its two major metabolites, noroxycodone and oxymorphone.

Materials and Methods

Materials

Human hepatocellular carcinoma cell lines (HepG2) cells were obtained from American Type Culture Collection (ATCC) (Manassas, VA). Rifampicin, omeprazole, β-naphthoflavone, dexamethasone, phenobarbital sodium salt, and dimethylsulfoxide (DMSO) were purchased from Sigma-Aldrich (St. Louis, MO). Lipofectamine 2000 transfection reagent was obtained from GIBCO/Invitrogen (Carlsbad, CA). Luciferase substrate (Steady-Glo) and Dual Luciferase Reporter Assay Systems were purchased from Promega (Madison, WI). Alamar blue (resazurin) was purchased from Trek Diagnostics (Chicago, IL); 6-(4-chlorophenyl)imidazo[2,1-b][1,3]thiazole-5-carbaldehyde *O*-(3,4-dichlorobenzyl oxime (CITCO) was purchased from Biomol Research Laboratories (Plymouth, PA). Oxycodone hydrochloride was generously donated by Dr. Andrew Coop (School of Pharmacy, University of Maryland, Baltimore), and noroxycodone and oxymorphone were purchased from Cerilliant Co. (Round Rock, TX). FuGENE 6 transfection reagent was obtained from Roche (Mannheim, Germany). Fetal bovine serum was purchased from Hyclone (Lonan, UT), whereas other cell culture reagents were from Invitrogen.

Plasmid Constructions

The pCR3-human CAR Human CAR expression vector and pCR3-mCAR (Mouse CAR expression vector) expression vectors were obtained from Dr. Masahiko Negishi (National Institutes of Health National Institute of Environmental Health Sciences). The CYP2B6-PBREM (phenobarbital-responsive enhancer module)/XREM (xenobiotic-responsive enhancer module) reporter construct was generated as reported previously (Wang et al., 2003). The rat PXR and human AhR-DRE transactivation kits were obtained from Puracyp (Carlsbad, CA). The generation of adenovirus containing EYFP (Enhanced yellow fluorescent protein)-tagged hCAR was described previously (Li et al., 2009). The pRL-Tk Thymidine kinase promoter-Renilla luciferase reporter construct used to normalize the firefly activity was purchased from Promega.

Experimental Animals

Male Sprague-Dawley rats (250–275 g; age, 8–9 weeks) were purchased from Harlan Laboratories (Indianapolis, IN). Female sex steroid hormones can induce protein expression (Campbell and Febbraio, 2002; Kim and Benet, 2004). As a result, males only were used to avoid potential influences on protein expression caused by fluctuations in ovarian hormone concentrations that are associated with different stages of the estrus cycle in females. They were fed chow and water ad libitum and maintained on a 12-hour light/dark cycle. The animals were housed individually and allowed to acclimate for at least one week before the experiments were conducted. The protocol for the animal studies was approved by the School of Pharmacy, University of Maryland Insitutional Animal Care and Use Committee.

Repeated Administration of Oxycodone

Sprague-Dawley rats were sorted into one of two groups (six per group) and were administered either a 15 mg/kg i.p. dose of oxycodone hydrochloride (dissolved in saline) or 1 ml/kg saline control twice daily every 12 hours for 8 days. Oxycodone treatment regimen was selected on the basis of reports that oxycodone is 1.5 times more potent than morphine (Kalso et al., 1990; Heiskanen et al., 1998; Nielsen et al., 2000), and a dose of 15 mg/kg oxycodone is equivalent to a dose of 20 mg/kg morphine, which is commonly used for morphine administration (Guitart and Nestler, 1989; Poyhia and Kalso, 1992; Aquilante et al., 2000; Ammon et al., 2003). Because oxycodone has an elimination half-life ($t_{1/2}$) of 3.0 $\pm$ 0.5 hours and requires five half-lives (>15 hours) for ~95% of the drug to be eliminated (Chan et al., 2008), twice daily administration (Holtman and Wala, 2006; Hassan et al., 2007, 2010) was used. Administration of drug every 12 hours ensures that enough oxycodone is administered before its complete elimination. Finally, an 8-day treatment regimen was adopted, because rats under similar experimental conditions developed tolerance to the analgesic effect of oxycodone (Hassan et al., 2007). The oxycodone-treated group was compared directly with saline-treated control, which was handled, treated, and sacrificed in parallel under the same experimental conditions.

Tissue Preparation and RNA Extraction

Rats in both groups were euthanized by carbon dioxide asphyxiation and decapitated 12 hours after administration of the last dose. Total RNA samples were isolated immediately from fresh liver tissues with use of TRIzol reagent (Qiagen, Valencia, CA), according to the manufacturer's instructions. The concentration of total RNA was measured by UV spectrophotometry at 260/280 nm. Thirty micrograms of total RNA was then subjected to DNase treatment of 10 minutes with use of the RNase-free DNase set (Qiagen), according to the manufacturer's instructions. Samples were then subjected to RNA clean-up with use of RNeasy MinElute Kit (Qiagen), according to the manufacturer's instructions. The concentration of purified RNA was measured by UV spectrophotometry, and RNA quality was assessed by electrophoresis on a 1% agarose gel. Further assessment of the integrity of the RNA was tested using an Agilent 2100 Bioanalyzer (Agilent Technologies, Palo Alto, CA). Only RNA samples with sharp and defined 28S and 18S ribosomal peaks indicating good RNA integrity were used.

Microarray Hybridization and Staining

A GeneChip rat genome 230 2.0 array (Affymetrix, Santa Clara, CA) containing 31,000 probe sets that analyze the expression level of over 30,000 transcripts encoding for over 28,000 well-substantiated rat genes was used to evaluate RNA expression. RNA samples (six liver tissue samples per group) were combined; thus, two RNA samples were pooled into one sample, resulting in a total of three pooled RNA samples per group. Pooled RNA samples from both groups were labeled and run on the arrays at the same time for each experiment (three arrays per group). In brief, total RNA (5 μg/array) was converted to cDNA, amplified, and labeled according to the Affymetrix protocols. Hybridization and washing were performed using the Affymetrix Fluidics Station 450 and Hybridization Oven 640 under standard conditions. The arrays were then scanned with a GeneChip Scanner 3000 (Affymetrix).

Microarray Data Analysis

Based on six individual Affymetrix CEL files (three/group), gene expression measures were calculated using the Background Adjusted Robust Multiple Average method (Wu et al., 2004) and implemented in the Bioconductor R packages *Affy* and *gcrma* (Gentleman et al., 2005). This process includes background correction, probe-level quantile normalization, and expression measures calculated by using median polish. A detection *P* value by Affymetrix Microarray suite, version 5, was used to make a reliable prediction of gene expression (present, marginal, or absent). Fold changes in the transcript levels and statistical analysis were calculated using Spotfire DecisonSite 8.2.1 algorithm (Spotfire Inc., Somerville, MA). Significance Analysis of Microarrays (Stanford University, Stanford, CA) was used to investigate differentially expressed genes. Then, we applied rigorous, conservative criteria to select candidate genes for further analysis as follows: (1) genes must have present or marginal calls in all arrays, (2) genes must have raw signals >40 in all arrays, (3) genes must be up/down regulated by ≥1.5-fold relative to the control, and (4) genes must have mean differences that are statistically significant ($P < 0.05$) from the control. Only genes that met the above criteria were considered to be significantly regulated and were used for further analysis. Under the above conditions, Affymetrix arrays have been shown to achieve a statistical power of >0.8 to detect 1.5-fold changes and >0.99 to detect 2.0-fold changes (Shippy et al., 2004). For each gene, fold change values were calculated by dividing normalized mean log-transformed probe set intensities of oxycodone-treated rats versus saline-treated rats.

qRT-PCR

Expression levels of 18 genes [14 significantly regulated ($P < 0.05$) and 4 nonsignificantly regulated ($P > 0.05$)] (Supplemental Table 1) were tested by qRT-PCR to validate the microarray findings. This approach was adopted to test the reliability of the normalization and statistical methods used for the microarray data analysis. qRT-PCR was conducted according to the manufacturer's recommendation with use of the iCycler instrument (Bio-Rad, Hercules, CA). In brief, 1 μg of total RNA was used to synthesize cDNA in a final reaction volume of 20 μl with use of the iScript reverse transcription kit (Bio-Rad). Two microliters of the reverse transcription reaction were used as template for qRT-PCR reactions, which were performed in a total volume of 25 μl with use of iQ SYBR Supermix (Bio-Rad) with a final primer concentration of 200 nM. Primers for qRT-PCR were designed using Beacon Designer software (Biosoft International, Palo Alto, CA). Primers were then tested for specificity by blasting the candidate sequence against the whole rat database (Annereau et al., 2004). Designing of primers was performed in an iterative fashion until a specific primer for each gene was obtained. After an initial denaturation step at 95°C for 3 minutes, PCR cycles ($n = 40$) consisted of a 30-second melt at 95°C, followed by annealing and extension at 60°C for 45 seconds. All reactions were conducted in triplicate. The threshold cycles (Ct) were calculated using the second derivative of the reaction and were automatically set by the iCycler iQ real time detection system software. The Ct of each gene was normalized against that of glyceraldhyde-3-phosphate dehydrogenase, which showed no change after oxycodone treatment in our microarray study. Fold changes were determined using the Livak method (δ-δ Ct method). The Student's *t* test was used to determine the statistical significance ($P < 0.05$) of the normalized Ct with use of SigmaStat statistical package, version 2.03 (Systat Software Inc., San Jose, CA).

Determination of the Protein Expression of Representative Metabolizing Enzymes (CYP3A1 and CYP2B2) and Transporter (ABCB1)

Preparation of Rat Hepatic Microsomes. Isolation of liver microsomes was adopted from standard procedures (van der Hoeven and Coon, 1974; Waxman, 1984). In brief, frozen liver tissue samples (three per group) from both treatment groups were rapidly thawed at 37°C and immediately homogenized with 2 volumes of 20 mM Tris-HCl (pH 7.4) buffer containing 1 mM DTT and 1 tablet (Complete Mini, EDTA-free protease inhibitor cocktail; Roche Diagnostics). After differential centrifugation, the final microsomal fraction was suspended in buffer containing 20 mM Tris-HCl (pH 7.4), 0.1 mM EDTA, and 20% glycerol and stored at −80°C until further analysis. Protein concentration was measured using bovine serum albumin as a standard in the Bio-Rad DC Protein Assay.

SDS-PAGE and Immunoblotting. SDS-PAGE and immunoblotting of representative metabolizing enzymes (CYP3A1 and CYP2B2) and the transporter (ABCB1) were conducted. CYP3A1 immunodetection was performed as previously described using the Laemmli discontinuous buffer system in a 10% polyacrylamide gel with a 5% stacking gel (Laemmli, 1970). Each well (three per group) was loaded with 40 μg of microsomal protein isolated from oxycodone- or saline-treated rats. In addition, 2 wells (controls) were loaded with 10 μg of standard rat liver microsomes purchased from BD Biosciences (San Jose, CA). Resolved proteins were transferred electrophoretically to Bio-Rad Immun-Blot polyvinylidene difluoride membranes. Polyvinylidene difluoride membranes were washed several times with Tris-buffered saline/Tween 20 washing buffer consisting of 1× Tris-buffered saline and 0.05% Tween 20 and incubated for 1 hour at 25°C in a solution of 5% nonfat dry milk in Tris-buffered saline/Tween 20 to block protein-binding sites. Membranes were incubated overnight at 4°C with antisera raised in rabbits against CYP3A1 (1:800 dilution) that was purchased from Abcam Inc. (Cambridge, MA). The polyvinylidene difluoride membrane was exposed to goat anti-rabbit IgG horseradish peroxidase (Santa Cruz Biotechnology, Santa Cruz, CA) at a dilution of 1:10,000. CYP2B2 microsomal protein was detected using 1.0 μg/ml mouse monoclonal anti-CYP2B2 antibody (Abcam) and goat anti-mouse secondary antibody (Santa Cruz Biotechnology). Immunoreactive protein was detected using the SuperSignal West Pico Chemiluminescent Substrate Kit (Pierce, Rockford, IL). The drug efflux transporter protein P-glycoprotein (ABCB1) was detected using a similar immunoblotting method with use of 1.3 μg/ml of mouse monoclonal Abcb1 antibody clone C219 (ID Laboratories, Inc., London, ON, Canada) and a goat anti-mouse IgG secondary antibody (Santa Cruz Biotechnology). Band density was quantified using densitometry with use of Quantity One 4.4.1 software (Bio-Rad). A separate membrane was used for immunoblotting of each protein. For protein normalization, each membrane was probed in an analogous fashion for immunoreactive β-actin with use of monoclonal anti-β-actin (1:5000) produced in mice (Sigma-Aldrich) and 1:10,000 dilution of goat anti-mouse IgG horseradish peroxidase (KPL, Gaithersburg, MD).

Gene Network Identification by the Computational Platform, MetaCore

MetaCore is a computational resource that uses logic operation algorithms to interpret changes in gene expression for a given condition in terms of biologic processes and molecular functions. Genes (XRs, transporters, and DMEs) in rat liver with altered expression (change, ≥1.5; $P < 0.05$) were characterized using Gene Ontology. Gene Ontology describes gene products in terms of their associated biologic processes, cellular components, and molecular functions. The Gene Ontology entries are hierarchically linked, thus allowing construction of cluster genes of crossed pathways. MetaCore also generates statistically significant gene networks. These networks represent gene interactions compiled from a curated database of rat protein interactions, metabolism, and bioactive compounds and, thus, provides a useful approach to identify new interactions/relationships with use of data obtained from numerous reported genomic studies (Ekins et al., 2006).

Many algorithms are integrated into MetaCore to enable construction and analysis of gene networks (Ekins et al., 2006). Because of the large number of selected genes (metabolic enzymes, nuclear receptors, and transporters) in the dataset, the Direct Interactions algorithm was used to create a gene network. Each connection between objects in the created network represents a direct, experimentally confirmed, physical interaction among the objects (Ekins et al., 2006). The Direct Interactions algorithm is advantageous when used for initial insight about the dataset, because it can determine whether uploaded genes in the list cluster together by interacting with each other (Ekins et al., 2006).

Transactivation Assays

Human PXR Transactivation Assay. For the human PXR transactivation assay, the methodology of Zhu et al. was used (Zhu et al., 2004). In brief, HepG2 cells were transfected with pcDNA3-hourPXR and pGLcyp2B6-Luc plasmids with use of Lipofectamine 2000. Oxycodone, noroxycodone, and oxymorphone (each dissolved in DMSO) were added to the wells of a 96-well plate at concentrations of 1–30 μM in triplicate (final concentration of DMSO was 0.5% v/v). Rifampicin (10 μM), a well-known hPXR agonist, was added to the plate as both a positive control and an internal standard. CITCO (1 μM), a known hCAR activator, was used as a negative control, and 0.5% DMSO was used as a blank control. The plate was incubated overnight at 37°C before the addition of luciferase substrate. After 30 minutes incubation with luciferase, the plate was read on a Packard TopCount plate reader (GMI Inc., Ramsey, MN) for luminescence intensity. Cytotoxicity was assessed using Alamar blue as previously described (Zhu et al., 2007).

Rat PXR and Human AhR-DRE Transactivation Assays. Culturing of the rat PXR and human AhR-DRE cell lines and transactivation assays were performed according to the manufacturer's instructions. In brief, cryopreserved cells were plated in 96-well plates and allowed to attach overnight before drug treatment. Oxycodone, noroxycodone, and oxymorphone were added at concentrations of 0.1–30 μM dissolved in DMSO (0.1% v/v). Dexamethasone (5 μM), a well-known rPXR agonist, and β-naphthoflavone, a well-known human AhR agonist, were added to the plates as positive controls; 0.1% DMSO was used as a blank control. After 24–48 hours of exposure to vehicle, compounds, and positive controls, the luminescent intensity was measured.

Human CAR and Mouse CAR Transactivation Assays. $HepG_2$ cells were cultured in 24-well plates in DMEM supplemented with 10% fetal bovine serum and antibiotics before transfection. Cells were cotransfected with 30 ng of nuclear receptor expression vector (mCAR or hCAR1+A), 60 ng of luciferase CYP2B6 reporter plasmids, and 10 ng of control plasmid (pRL-TK) with use of FuGENE 6 reagent, according to the manufacturer's protocol. After 18 hours of transfection, cells were treated for 24 hours in triplicate with oxycodone, noroxycodone, and oxymorphone at concentrations of 1–30 μM. CITCO (1 μM) or TCPOBOP 1,4-Bis[2-(3,5-dichloropyridyloxy)]benzene (250–500 nM) was used as positive control for hCAR and mCAR, respectively, and rifampicin (10 μM), the hPXR agonist, was used as a negative control in the hCAR assay. Cell lysates were assayed for firefly luciferase activities and normalized against the activities of cotransfected Renilla luciferase. Ratios of the two luciferase activities were expressed as fold activation relative to the vehicle control.

Translocation of Ad/EYFP-hCAR in Human Primary Hepatocyte Cultures

Liver tissue samples were obtained by qualified medical staff after donor consent and prior approval from the Institutional Review Board at the University of Maryland at Baltimore. Isolation of human hepatocytes was performed in accordance with the two-step collagenase method described previously (LeCluyse et al., 2005). Human hepatocytes donated by a 77-year-old female were seeded at 3.75×10^5 cells/well in 24-well biocoat plates and cultured as described previously (Wang et al., 2003). Twenty-four hours later, hepatocyte cultures were infected with Ad/EYFP-hCAR for 12 hours before treatment with vehicle control (0.1% DMSO), phenobarbital (1000 μM), or oxycodone (30 μM) for another 12 hours. Then, the subcellular localization of Ad/EYFP-hCAR was visualized by confocal laser scanning microscopy with use of a Nikon C1-LU3 instrument based on an inverted Nikon Eclipse TE2000 microscope (Mellville, NY).

Results

Oxycodone-Induced Gene Expression Changes in Liver Tissue of Sprague-Dawley Rats. For the oxycodone-treated rats, no behavioral or withdrawal effects were noticed during or after oxycodone treatment except for the common opioid-induced Straub tail effects. Using a microarray approach, we examined the effect of repeated oxycodone administration on gene expression in liver tissue of Sprague-Dawley rats. Considering all 31,000 probe sets (gene identifiers) corresponding to 28,000 genes represented on each array, oxycodone treatment significantly ($P < 0.05$) induced changes in 1973 probe sets (~6% of probe sets), of which, 670 probe sets had P values <0.01 (unpublished data). Among those 670 probe sets, 140 gene identifiers (corresponding to 130 genes) were up/down-regulated by ≥2-fold [68 gene identifiers were upregulated by ≥2-fold (Supplemental Table 2), and 72 gene identifiers were downregulated by ≥2-fold (Supplemental Table 3)]. Three XRs (PXR, CAR, and AhR) were significantly ($P < 0.05$) upregulated by 2.9 ± 0.02–fold, 6.1 ± 0.1–fold, and ~2.3 ± 0.2–fold, respectively (Table 1). Twenty-nine probe sets (Table 2) encoding 27 transporters were significantly ($P < 0.05$) altered with fold changes ranging from −46.3 to 3.6. Five of these transporters belong to the ATP binding cassette (ABC) superfamily (e.g., ABCB1 and ABCB4), and the remainder belong to the Solute Linked Carrier (SLC) superfamily (e.g., SLC16A1 and SLC22A8) (Table 2). On the other hand, 22 probe sets encoding 19 metabolizing enzymes (e.g., CYP2B2, CYP3A1, and UGTA1) were significantly ($P < 0.05$) altered, with fold changes ranging from −3.3 to 17.1 (Table 3). Significance Analysis of Microarrays–based statistical analysis of the microarray data revealed a minimal false discovery rate of <0.01, indicating the presence of <1% chance of false positives in the microarray data (unpublished data).

Validation of Microarray Data by qRT-PCR. To validate the microarray data, the expression levels of 14 significantly ($P < 0.05$) and 4 nonsignificantly ($P > 0.05$) regulated genes (as determined by the microarray analysis) were analyzed using qRT-PCR analysis. After ascertaining the amplicon specificity by first-derivative melting curve analysis, the values obtained for each gene were normalized to the values of the corresponding glyceraldhyde-3-phosphate dehydrogenase expression. All significantly ($n = 14$) and nonsignificantly ($n = 4$)

TABLE 1

Significantly regulated xenobiotic receptors in liver tissues of oxycodone-treated rats

Fold change values are expressed as mean ± S.D. (n = 3). Metacore-assigned gene symbols/names are indicated in parentheses (column 1) if different from Affymetrix gene symbols/names.

Gene Symbol	Gene Title	Fold Change	*P* Value	GenBank Accession No.
NR1I3 (CAR)	Nuclear receptor subfamily 1, group I, member 3	6.1 ± 0.1	0.002	NM_022941
NR1I2 (PXR)	Nuclear receptor subfamily 1, group I, member 2	2.9 ± 0.02	0.001	NM_052980
AhR[a]	Aryl hydrocarbon receptor	2.3 ± 0.1	0.002	AA858521
		2.2 ± 0.3	0.004	

[a] Gene represented twice in the microarray chips.

TABLE 2

Differentially expressed transporters in liver tissues of oxycodone-treated rats

Fold change values are expressed as mean ± S.D. (n = 3). Metacore-assigned gene symbols/names are indicated in parentheses (column 1) if different from Affymetrix gene symbols/names.

Gene Symbol	Gene Title	Fold Change	*P* Value	GenBank Accession No.
Abcg5	ATP-binding cassette, sub-family G (WHITE), member 5	3.6 ± 0.1	0.004	NM_053754
Abcb1a[a] (MDR1)	ATP-binding cassette, sub-family B (MDR/TAP), member 1A	3.6 ± 0.1	0.005	AY582535
Slc16a10	Solute carrier family 16 (monocarboxylic acid transporters), member 10	3.0 ± 0.03	0.008	AB047324
Slc22a5	Solute carrier family 22 (organic cation transporter), member 5	2.8 ± 0.1	0.013	NM_019269
Abcb1a (MDR1)	ATP-binding cassette, sub-family B (MDR/TAP), member 1A	2.8 ± 0.1	0.002	AY582535
Slc1a2	Solute carrier family 1 (glial high affinity glutamate transporter), member 2	2.4 ± 0.2	0.015	NM_017215
*Abca8b*_predicted	ATP-binding cassette, sub-family A (ABC1), member 8b (predicted)	2.3 ± 0.02	0.001	BF386852
Slc25a15[a] _predicted	Solute carrier family 25 (mitochondrial carrier; ornithine transporter) member 15 (predicted)	2.2 ± 0.01	0.009	BF554040
*Slc25a15*_predicted	Solute carrier family 25 (mitochondrial carrier; ornithine transporter) member 15 (predicted)	2.1 ± 0.01	0.005	BG377383
Slc37a4 (G6PT1)	Solute carrier family 37 (glycerol-6-phosphate transporter), member 4	2.0 ± 0.01	0.019	NM_031589
Slc38a4	Amino acid transport system A3	1.8 ± 0.01	0.007	NM_130748
Slc27a5	Bile acid CoA ligase	1.6 ± 0.02	0.005	NM_024143
*Slc39a4*_predicted	Solute carrier family 39 (zinc transporter), member 4 (predicted)	1.6 ± 0.01	0.012	AI556941
*Slc17a5*_predicted	Solute carrier family 17 (anion/sugar transporter), member 5 (predicted)	1.5 ± 0.01	0.005	AA900983
Abcb4 (MDR3)	ATP-binding cassette, sub-family B (MDR/TAP), member 4	1.5 ± 0.03	0.049	NM_012690
Slc21a10	Solute carrier family 21, member 10	1.5 ± 0.02	0.029	AF147740
Slc2a2	Solute carrier family 2 (facilitated glucose transporter), member 2	1.5 ± 0.01	0.003	NM_012879
*Slc25a29*_predicted	Solute carrier family 25 (mitochondrial carrier, palmitoylcarnitine transporter), member 29 (predicted)	1.5 ± 0.04	0.034	BF555120
Slc6a9	Solute carrier family 6 (neurotransmitter transporter, glycine), member 9	−1.6 ± 0.02	0.038	AA943735
Abcg1	ATP-binding cassette, sub-family G (WHITE), member 1	−1.7 ± 0.04	0.020	NM_053502
Slc25a30	Solute carrier family 25, member 30	−1.8 ± 0.01	0.038	H35736
Slc16a1	Solute carrier family 16 (monocarboxylic acid transporters), member 1	−1.9 ± 0.04	0.033	NM_012716
Slc35b2	Solute carrier family 35, member b2	−2.2 ± 0.1	0.006	BI293600
*Slc41a2*_predicted	Solute carrier family 41, member 2 (predicted)	−2.5 ± 0.1	0.030	BF410740
Slc15a3	Peptide/histidine transporter PHT2	−2.6 ± 0.1	0.006	AB026665
Slc7a7	Solute carrier family 7 (cationic amino acid transporter, y+ system), member 7	−2.8 ± 0.2	0.031	AF200684
Slc10a2	Solute carrier family 10, member 2	−6.3 ± 0.8	0.001	NM_017222
Slc34a2	Solute carrier family 34 (sodium phosphate), member 2	−6.6 ± 0.4	0.023	NM_053380
Slc22a8	Solute carrier family 22 (organic anion transporter), member 8	−46.3 ± 2.2	0.001	NM_031332

[a] Genes represented more than once.

regulated genes as indicated by the microarray analysis showed similar patterns (comparable fold changes and *P* values) after evaluation of their expression levels with use of qRT-PCR analysis (i.e., qRT-PCR data were comparable to the microarray data). Computation of Pearson correlation coefficients (for the 14 significantly regulated genes) indicated that there was a significant ($r = 0.973$; $P < 0.0000001$) correlation between the qRT-PCR and the microarray data (unpublished data). For the four nonsignificantly regulated genes, there was also a significant correlation between fold changes obtained from microarray analysis and qRT-PCR ($r=0.956$; $P < 0.043$) (unpublished data). These results confirm the validity of the microarray data and give confidence in the normalization and the statistical methods used for the microarray data analysis.

Influence of Repeated Oxycodone Administration on the Protein Expression of Representative Metabolizing Enzymes (CYP3A1 and CYP2B2) and Transporter (ABCB1). To further validate the microarray data, protein expression of key DMEs and efflux transporter that play major roles in mediating DDIs (Weinstein and Gaylord, 1979; Lin, 2003; Yue et al., 2009; Choi et al., 2010; Giacomini et al., 2010; Calcagno et al., 2012) were determined. Western blot analyses identified CYP3A1 protein (57-59 kDa) in liver samples isolated from saline, oxycodone, and standard rat liver microsomes. The optical density calculations (mean ± S.D., $n = 3$) of CYP3A1 bands after normalization to β-actin for saline and oxycodone groups were 6.0 ± 2.9 and 12.2 ± 1.4, respectively ($P < 0.01$) (unpublished data). This indicates a significant upregulation (2.0-fold) in CYP3A1 protein levels in oxycodone-treated rats that was comparable with fold changes obtained from the microarray (1.7-fold) and the qRT-PCR (2.7-fold) analyses. In addition, the normalized optical density calculations (mean ± S.D., $n = 3$) of CYP2B2 protein bands (56 kDa) were 0.18 ± 0.05 and 0.84 ± 0.15 for saline and oxycodone samples, respectively ($P < 0.001$) (unpublished data). These results demonstrate that CYP2B2 protein expression was significantly induced by ~5.0-fold in oxycodone-treated rats, consistent with the microarray (6.0-fold) and the qRT-PCR (5.8-fold) data. Finally, ABCB1 protein was identified around 168–170 kDa, with normalized optical density values (mean ± S.D., $n = 3$) of 0.38 ± 0.09 and 1.2 ± 0.3 for saline and oxycodone samples, respectively ($P < 0.01$) (unpublished data). This indicates upregulation of ABCB1 (~3.0-fold) in oxycodone-treated rats, consistent with the microarray (~3.2-fold), qRT-PCR (4.0-fold), and our previously reported study (4.0-fold) (Hassan et al., 2007).

Identification of Cause-Effect Relationship among XRs, Transporters, and DMEs by MetaCore. Genes that were significantly ($P < 0.05$) up/downregulated by at least 1.5-fold (Tables 1–3) were uploaded into MetaCore. Using Direct Interactions algorithm, we identified a unique cluster of interacting gene-encoded proteins representing XRs, transporters, and DMEs. Only genes that exhibit one or more interaction are shown. Noninteracting genes were omitted from the figure, because they do not reveal possible cause-effect relationships (Fig. 1). The corresponding subnetwork was assembled around PXR, CAR, and AhR, showing direct interactions among genes and revealing potential cause-effect relationships. In the network, positive interactions are indicated by green hexagons [e.g., interaction between PXR and MDR (multidrug resistance protein) 1 (ABCB1)], negative interactions are indicated by red hexagons (e.g., interaction between CAR and CYP2E1), and unspecified interactions are indicated by black hexagons (e.g., interaction between AhR and MDR1) (Fig. 1). Each of these interactions/relationships represents validated, experimentally confirmed interactions (Ekins et al., 2006). Differentially

TABLE 3

Differentially expressed metabolizing enzymes in liver tissues of oxycodone-treated rats

Fold change values are expressed as mean ± S.D. (n = 3). Metacore-assigned gene symbols/names are indicated in parentheses (column 1) if different from Affymetrix gene symbols/names.

Gene Symbol	Gene Title	Fold Change	*P* Value	GenBank Accession No.
CYP17a1[a]	Cytochrome P450, family 17, subfamily a, polypeptide 1	17.1 ± 1.3	0.004	NM_012753
Por[a,b] (cytochrome P450 reductase)	Cytochrome P450 oxidoreductase	8.4 ± 0.03	0.001	NM_031576
Por (cytochrome P450 reductase)	Cytochrome P450 oxidoreductase	7.0 ± 0.1	0.002	NM_031576
Yc2 // Gsta5[a]	Glutathione S-transferase Yc2 subunit	7.0 ± 0.6	0.001	AA945082
CYP2b2[a]	Cytochrome P450, family 2, subfamily b, polypeptide 2	6.0 ± 0.02	0.008	AI454613
FMO1[a]	Flavin containing monooxygenase 1	3.7 ± 0.1	0.010	NM_012792
Ces2[a]	Carboxylesterase 2 (intestine, liver)	2.8 ± 0.02	0.001	NM_133586
CYP2j4	Cytochrome P450, family 2, subfamily J, polypeptide 4	2.4 ± 0.01	0.001	NM_023025
Ugt1a1[b] (UGT)	UDP glycosyltransferase 1 family, polypeptide A1	2.0 ± 0.02	0.026	AF461738
CYP4a10	Cytochrome P450, family 4, subfamily a, polypeptide 10	2.0 ± 0.04	0.027	NM_016999
CYP27a1	Cytochrome P450, family 27, subfamily a, polypeptide 1	1.9 ± 0.03	0.003	M73231
CYP4b1	Cytochrome P450, family 4, subfamily b, polypeptide 1	1.9 ± 0.03	0.004	M29853
CYP2a1	Cytochrome P450, family 2, subfamily a, polypeptide 1	1.7 ± 0.04	0.002	NM_012692
CYP3a1(CYP3A4)[a]	Cytochrome P450, family 3, subfamily a, polypeptide 1	1.7 ± 0.01	0.026	NM_173144
Ugt1a1 (UGT)	UDP glycosyltransferase 1 family, polypeptide A1	1.6 ± 0.02	0.025	AF461738
CYP2e1	Cytochrome P450, family 2, subfamily e, polypeptide 1	1.5 ± 0.01	0.009	NM_031543
CYPbb[b]	Cytochrome b_{245}, βpolypeptide	−2.0 ± 0.02	0.017	BE098739
CYPba	Cytochrome b_{245}, αpolypeptide	−2.0 ± 0.02	0.018	AI232788
CYPbb	Cytochrome b_{245}, βpolypeptide	−2.1 ± 0.05	0.018	BE098739
CYP2c	Cytochrome P450, family 2, subfamily c	−2.1 ± 0.04	0.003	NM_019184
CYP2c13[a]	Cytochrome P450, family 2, subfamily c, polypeptide 13	−2.2 ± 0.04	0.002	J02861
Sult1a2	Sulfotransferase family 1A, member 2	−3.3 ± 0.03	0.001	NM_031732

[a] Previously reported genes (Myers et al., 2010).
[b] Genes represented more than once.

expressed genes can be visualized simultaneously and identified by expression signs at the top right of each node, where red small circles indicate up-regulation (Fig. 1) and blue small circles indicate down-regulation (not shown in the figure, because no interactions with other genes were detected). In addition to showing the interactions between each XR and the regulated transporters and DMEs, the MetaCore-generated network also shows the intra-relationships among XRs (Fig. 1). It indicates that XRs can interact and, perhaps, regulate each other (e.g., positive interaction between PXR and AhR), consistent with previous reports (Tirona and Kim, 2005). Of interest, the MetaCore analysis also indicated that the transcription factor FKHR (upregulated by 2.9-fold, $P < 0.001$) (Supplemental Table 2) may also be involved in modulating many XRs, transporters, and DMEs (e.g., PXR, CAR, MDR1, and CYP2B6) (Fig. 1).

Transactivation/Translocation Assays. To identify whether oxycodone or its two main metabolites (noroxycodone or oxymorphone) can activate XRs we conducted a series of cell-based transactivation assays. For rPXR, hPXR, hAhR, and mCAR, all positive control compounds responded appropriately in each transactivation assay (Fig. 2). Neither oxycodone nor its metabolites demonstrated significant ($P > 0.05$) transactivation in any assay up to a concentration of 30 μM. In contrast to other receptors, hCAR is constitutively activated in all immortalized cell lines and is insensitive to chemical stimulation even by the hCAR agonist, CITCO (Fig. 2E). As a result, hCAR1+A–transfected cells were used. Oxycodone and its metabolites did not activate hCAR1+A (Fig. 2F).

Recently, chemical-mediated nuclear translocation of hCAR in human primary hepatocyte cultures was established as a novel tool for

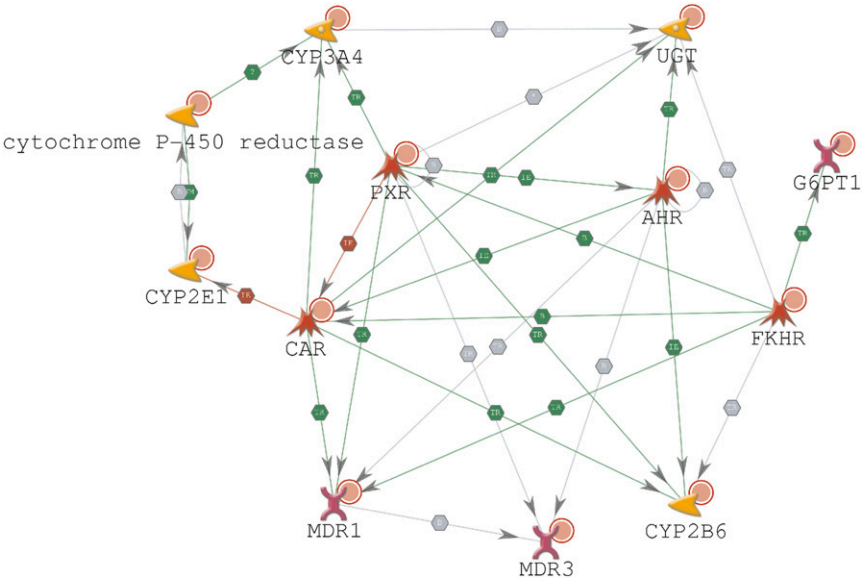

Fig. 1. Gene network of interactions among differentially expressed genes encoding XRs, transporters, and DMEs resulting from oxycodone treatment, compared with saline treatment, in liver tissue samples of Sprague-Dawley rats. Gene network was obtained using MetaCore after applying the Direct Interactions algorithm. Only genes that exhibit one or more interactions with others are shown. Genes without direct interactions were omitted from the figure, because they do not reveal cause-effect relationships. Colored, highlighted symbols (nodes) represent genes. Red, small, solid circles (top right of each node) correspond to genes with significant ($P < 0.05$) up-regulation of ≥1.5-fold. The small, colored hexagons on vectors between nodes describe functional interactions. For example, positive interactions are indicated by green hexagons (e.g., interaction between PXR and MDR1), negative interactions are indicated by red hexagons (e.g., interaction between CAR and CYP2E1), and unspecified interactions are indicated by black hexagons (e.g., interaction between AhR and MDR1). Each connection (vector) represents a direct, experimentally confirmed, physical interaction between genes (Ekins et al., 2006). Red cone-like shapes represent XRs, purple X-like shapes represent transporters, and yellow arrows represent DMEs.

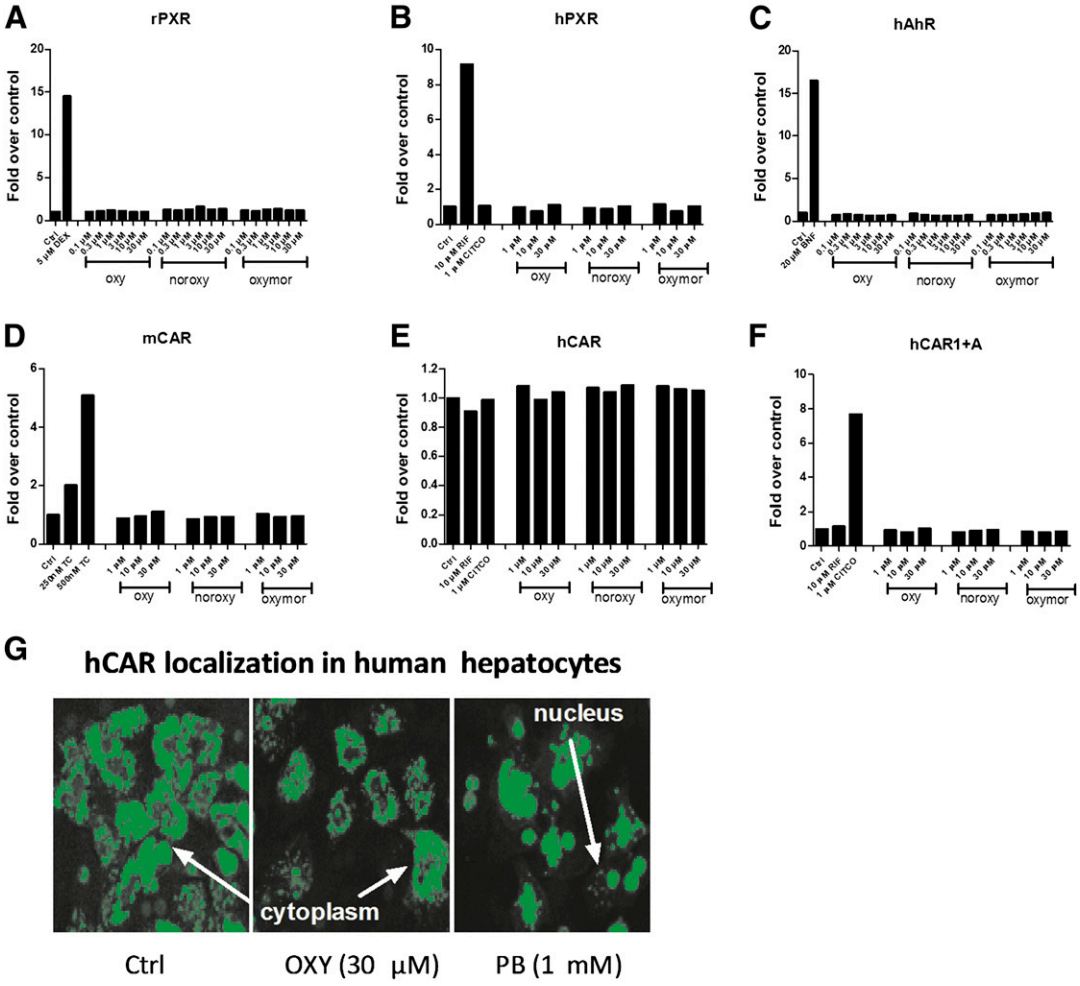

Fig. 2. Oxycodone (oxy), noroxycodone (noroxy), and oxymorphone (oxymor) are not activators of PXR, CAR, or AhR in cell-based experiments. HepG2 cells were cotransfected with CYP2B6 or CYP3A4 luciferase reporter plasmid, along with one of the XR expression vectors: rPXR (A), hPXR (B), hAhR (C), mCAR (D), hCAR (E), or hCAR1+A (F). After the transfections, cells were treated with oxy, noroxy, oxymor, or the corresponding positive or negative controls, as indicated in the figure. After treatment, luciferase activities were determined and expressed relevant to vehicle control. Data represent mean ± S.D. of three independent transfections. For the hCAR translocation assay (G), human primary hepatocytes were infected with Ad/EYFP-hCAR as described in Materials and Methods and treated with a vehicle control (0.1% DMSO), oxycodone (30 μM), or phenobarbital (1 mM). Then, the hepatocytes were subjected to analysis by confocal laser scanning microscopy, which indicated that translocation of hCAR to the nucleus occurred in response to phenobarbital but not oxy treatment.

predicting in vitro CAR activation (Li et al., 2009). Therefore, we conducted additional experiments to evaluate the ability of oxycodone to mediate translocation of hCAR in this model. As depicted in Fig. 2G, Ad/EYFP-hCAR is predominantly expressed in the cytoplasm of human primary hepatocytes before activation and accumulated in the nucleus in the presence of phenobarbital, a known hCAR activator. In contrast, oxycodone treatment (30 μM) did not translocate hCAR from the cytoplasm to the nucleus, which confirmed the inability of oxycodone to activate hCAR.

Discussion

The objective of this study was to evaluate the influence of repeated oxycodone administration on the expression of XRs, transporters, and DMEs. The results reported here demonstrate that oxycodone indeed modulates the expression of XRs (e.g., PXR, CAR, and AhR), transporters (e.g., ABCB1 and SLC16A1), and DMEs (e.g., CYP3A1 and CYP2B2) (Tables 1–3) as well as many other genes (Supplemental Tables 2 and 3). These findings are supported and validated. First, qRT-PCR analyses of 18 genes demonstrated a strong correlation between qRT-PCR and microarray data. Second, Western blot analysis of representative transporter (ABCB1) and DMEs (CYP3A1 and CYP2B2) confirmed the mRNA data. Third, we identified here several oxycodone-regulated genes (Supplemental Table 2; Table 2) that were previously reported in response to oxycodone and/or morphine (μ-opioid agonist similar to oxycodone; e.g., ABCB1, SLC16A1, SLC22A8, SLC1A2, SLC37A4, FKBP5, and ADAMTS1) (Aquilante et al., 2000; Homayoun et al., 2003; McClung et al., 2005; Hassan et al., 2010). Finally, our previous report (Hassan et al., 2007) supports the present data and demonstrates that ABCB1 was upregulated in liver tissue of oxycodone-treated rats. Collectively, these factors confirm the validity of the gene sets described in this study.

Twenty-seven transporters were significantly regulated by oxycodone (Table 2). The number of transporters altered by oxycodone underscores the importance of understanding the impact of concomitant administration of analgesics with other drugs. Five of these transporters belong to the ABC superfamily (e.g., ABCB1 and ABCB4). The efflux transporter ABCB1 was significantly upregulated (Table 2). This is consistent with our previous report (Hassan et al., 2007), in

which a lower dose of oxycodone (5 mg/kg) upregulated ABCB1 and impeded the accumulation of paclitaxel (ABCB1 marker) in liver tissue of oxycodone-treated rats. Paclitaxel is a chemotherapeutic agent often used for the management of hepatic cancer (Tono et al., 2004). Thus, our results raise the possibility that the coadministration of paclitaxel with oxycodone may diminish the chemotherapeutic effect of paclitaxel. Of note, oxycodone is an ABCB1 substrate (Hassan et al., 2007). Thus, the upregulation of ABCB1 could be a defensive mechanism to enhance oxycodone elimination, which in turn, can contribute to tolerance development to its analgesic activity.

The other altered transporters belong to the SLC superfamily (e.g., SLC22A8 and SLC16A1). A major finding of this study is dramatic downregulation of the organic anion transporter SLC22A8 (OAT3) by >46-fold. SLC22A8 is a transporter of special interest, because it transports a wide spectrum of substrates, including anticancer agents, antiretroviral agents, organic anions, and organic cations (Giacomini et al., 2010). SLC22A8 is reported to be involved in clinical DDI (Giacomini et al., 2010). If any of the SLC22A8 substrates (e.g., methotrexate, adefovir, cidofovir, and penicillin G) (Vanwert et al., 2007; VanWert and Sweet, 2008; Giacomini et al., 2010) are coadministered with oxycodone, their excretion could be impeded, which may lead to toxic levels in the plasma. As such, our data would suggest that coadministered drugs with oxycodone should be tested for SLC22A8 substrate specificity before their prescription.

Another notable SLC transporter altered by oxycodone treatment was SLC16A1 (Table 2). SLC16A1 is a proton-linked monocarboxylate transporter that transports lactates, pyruvates, mevalonates, and branched-chain oxo acids derived from leucine, isoleucine, and valine across plasma membranes (Fang et al., 2006). It regulates intracellular pH via symporting protons along with monocarboxylates. SLC16A1 was downregulated in both hepatic (Table 2) and brain tissues (Hassan et al., 2010). Downregulation of SLC16A1 results in acidic intracellular environment and affects many vital physiologic processes (e.g., protein folding, ligand binding, enzyme activity, and metabolism) that could lead to cell death (Fang et al., 2006). Therefore, our findings suggest that the apoptosis commonly observed in opioid-treated rodents could be, in part, attributable to SLC16a1 downregulation (Emeterio et al., 2006).

DMEs also play a critical role in the disposition of drugs and are involved in DDIs. Numerous DMEs were dramatically altered by oxycodone treatment (Table 3). For example, cytochrome P450 oxidoreductase (POR) and CYP17A1 (17α-hydroxylase/17,20-lyase) were strikingly upregulated by 8- and 17-fold, respectively. POR plays a pivotal role in facilitating electron transfer from reduced nicotinamide adenine dinucleotide phosphate to microsomal cytochrome P450 enzymes, including the steroidogenic enzymes CYP17A1, which plays a crucial role in androgens biosynthesis. Excessive androgen production is involved in the pathogenesis of serious diseases, including prostate cancer and benign prostatic hyperplasia (Bostwick et al., 1992). The induction of POR and CYP17A1 in oxycodone-treated male rats may trigger excessive androgen production.

Our data also indicate a potential risk for drug users. For instance, CYP2B2 and flavin containing monooxygenase (FMO) were significantly upregulated (Table 3). CYP2B2 plays a key role in the metabolism of cocaine to norcocaine (Boelsterli et al., 1992; Jover et al., 1993), and FMO facilitates the conversion of norcocaine to the hepatotoxic norcocaine nitroxide (Kloss et al., 1982). Our results signify a potential risk of serious hepatic injury if drug users coadminister cocaine with oxycodone, where upregulation of CYP2B2 and FMO by oxycodone may accelerate the formation of the hepatotoxic norcocaine nitroxide metabolite (Cone et al., 2003).

CYP3A1 is involved in the metabolism of many therapeutic agents (e.g., paclitaxel, morphine, and efavirenz) and is also responsible for *N*-demethylation of oxycodone. In fact, more than 80% of oxycodone administered dose undergoes CYP3A1-mediated *N*-demethylation to the inactive metabolite noroxycodone in rats (Weinstein and Gaylord, 1979). Likewise, CYP3A4 (human CYP3A1 isoform)–mediated *N*-demethylation in humans is the major oxidative pathway for oxycodone metabolism (Lalovic et al., 2006). Our results indicate that CYP3A1 was significantly upregulated (Table 3) by oxycodone, which could enhance noroxycodone formation. We hypothesize that CYP3A1 upregulation coupled with ABCB1 upregulation (Table 2) could be an adaptive mechanism that enhances the hepatic elimination of oxycodone and contributes to tolerance development to its analgesic effect (Hassan et al., 2007).

Another important aspect of this study was the induction of three key XRs (PXR, CAR, and AhR) by oxycodone (Table 1). MetaCore analysis (Fig. 1) generated a signature network of hepatic genes assembled around XRs in response to oxycodone administration and demonstrated that XRs, in addition to FKHR, a transcription factor, have direct regulatory effects on the transcription of many transporters and DMEs. To our knowledge, this is the first report to present a signature gene network in response to opioid treatment that provides insight into hepatic regulatory mechanisms associated with oxycodone treatment. Of particular interest are the interactions among MDR1 (ABCB1) and the XRs (PXR, CAR, AhR, and FKHR[Forkhead box O1A]), suggesting that oxycodone-induced upregulation of ABCB1 may result from the activation of PXR, CAR, AhR, and/or FKHR. Neither oxycodone nor its metabolites were capable of activating any of the tested XRs (Fig. 2). Morphine (structurally similar to oxycodone) demonstrated oxycodone-like characteristics, by which it induced the expression (unpublished data) but not the activity of hPXR and hCAR (Li et al., 2010). Likewise, the insulin-like growth factor-1 receptor inhibitor, BMS-665351, induced CYP3A4 and hCAR but did not activate hCAR or hPXR (Li et al., 2012). In summary, these results indicate that the observed induction of transporters/DMEs is not attributable to the direct activation of PXR, CAR, or AhR via oxycodone or its two major metabolites but, alternatively, could be attributable to activation of the induced PXR, CAR, and AhR via thus far unrecognized endogenous activators and/or an untested oxycodone metabolite.

In conclusion, this is the first report, to our knowledge, to elucidate the effect of repeated administration of an opioid on global gene expression in rat liver. Our findings demonstrate that oxycodone alters the expression of many drug disposition–controlling genes, including 3 XRs, 27 transporters, and 19 DMEs. The significance of these findings is 4-fold; first, it helps in explaining the escalating problem of DDIs when oxycodone is coadministered with substrates/inhibitors of these transporters/DMEs. Many of these DDIs have resulted in fatalities (Burrows et al., 2003; Cone et al., 2003, 2004; Nieminen et al., 2009). Second, oxycodone is often prescribed for medical conditions that involve moderate to severe pain. Our results underscore the importance of adjusting the therapeutic doses of substrates of the regulated transporters/DMEs that are coprescribed with oxycodone for management of these conditions. Third, our findings suggest that oxycodone may indirectly expedite its own elimination via enhancing both its hepatic efflux (through ABCB1 upregulation) and its hepatic metabolism to the inactive metabolite, noroxycodone (through upregulation of CYP3A1). These changes could be underlying mechanisms by which tolerance occurs to its analgesic effect. Finally, although regulation of transporters/DMEs is not attributable to direct activation of XRs via oxycodone or its two major metabolites, coadministration of XRs activators (e.g., methadone) with oxycodone

(XRs inducer) by drug addicts/users could lead to synergistic effects on XRs-mediated induction of transporters/DMEs that could lead to deleterious DDIs. We acknowledge that there are species differences between rats and humans, and as a result, these findings should be interpreted with caution when translated to humans.

Acknowledgments

The authors thank Dr. Hegang Chen for statistical consultation, and Jean Simmermacher-Mayer for some experimental efforts.

Authorship Contributions

Participated in research design: Hassan, Lee, H. Wang, Sinz, Eddington.

Conducted experiments: Hassan, Myers, Lee, D. Wang, Sinz.

Performed data analysis: Hassan and Mason.

Wrote or contributed to writing of the manuscript: Hassan, Lee, H. Wang, Sinz, Eddington.

References

Ammon S, Mayer P, Riechert U, Tischmeyer H, and Höllt V (2003) Microarray analysis of genes expressed in the frontal cortex of rats chronically treated with morphine and after naloxone precipitated withdrawal. *Brain Res Mol Brain Res* **112**:113–125.

Annereau JP, Szakács G, Tucker CJ, Arciello A, Cardarelli C, Collins J, Grissom S, Zeeberg BR, Reinhold W, and Weinstein JN, et al. (2004) Analysis of ATP-binding cassette transporter expression in drug-selected cell lines by a microarray dedicated to multidrug resistance. *Mol Pharmacol* **66**:1397–1405.

Aquilante CL, Letrent SP, Pollack GM, and Brouwer KL (2000) Increased brain P-glycoprotein in morphine tolerant rats. *Life Sci* **66**:PL47–PL51.

Boelsterli UA, Lanzotti A, Göldlin C, and Oertle M (1992) Identification of cytochrome P-450IIB1 as a cocaine-bioactivating isoform in rat hepatic microsomes and in cultured rat hepatocytes. *Drug Metab Dispos* **20**:96–101.

Bostwick DG, Cooner WH, Denis L, Jones GW, Scardino PT, and Murphy GP (1992) The association of benign prostatic hyperplasia and cancer of the prostate. *Cancer* **70**(1, Suppl) 291–301.

Burrows DL, Hagardorn AN, Harlan GC, Wallen ED, and Ferslew KE (2003) A fatal drug interaction between oxycodone and clonazepam. *J Forensic Sci* **48**:683–686.

Calcagno A, D'Avolio A, Simiele M, Cusato J, Rostagno R, Libanore V, Baietto L, Siccardi M, Bonora S, and Di Perri G (2012) Influence of CYP2B6 and ABCB1 SNPs on nevirapine plasma concentrations in Burundese HIV-positive patients using dried sample spot devices. *Br J Clin Pharmacol* **74**:134–140.

Campbell SE and Febbraio MA (2002) Effect of the ovarian hormones on GLUT4 expression and contraction-stimulated glucose uptake. *Am J Physiol Endocrinol Metab* **282**:E1139–E1146.

Chan S, Edwards SR, Wyse BD, and Smith MT (2008) Sex differences in the pharmacokinetics, oxidative metabolism and oral bioavailability of oxycodone in the Sprague-Dawley rat. *Clin Exp Pharmacol Physiol* **35**:295–302.

Choi YH, Lee U, Lee BK, and Lee MG (2010) Pharmacokinetic interaction between itraconazole and metformin in rats: competitive inhibition of metabolism of each drug by each other via hepatic and intestinal CYP3A1/2. *Br J Pharmacol* **161**:815–829.

Cone EJ, Fant RV, Rohay JM, Caplan YH, Ballina M, Reder RF, and Haddox JD (2004) Oxycodone involvement in drug abuse deaths. II. Evidence for toxic multiple drug-drug interactions. *J Anal Toxicol* **28**:616–624.

Cone EJ, Fant RV, Rohay JM, Caplan YH, Ballina M, Reder RF, Spyker D, and Haddox JD (2003) Oxycodone involvement in drug abuse deaths: a DAWN-based classification scheme applied to an oxycodone postmortem database containing over 1000 cases. *J Anal Toxicol* **27**: 57–67, discussion 67.

Ekins S, Bugrim A, Brovold L, Kirillov E, Nikolsky Y, Rakhmatulin E, Sorokina S, Ryabov A, Serebryiskaya T, and Melnikov A, et al. (2006) Algorithms for network analysis in systems-ADME/Tox using the MetaCore and MetaDrug platforms. *Xenobiotica* **36**:877–901.

Emeterio EP, Tramullas M, and Hurlé MA (2006) Modulation of apoptosis in the mouse brain after morphine treatments and morphine withdrawal. *J Neurosci Res* **83**:1352–1361.

Fang J, Quinones QJ, Holman TL, Morowitz MJ, Wang Q, Zhao H, Sivo F, Maris JM, and Wahl ML (2006) The H+-linked monocarboxylate transporter (MCT1/SLC16A1): a potential therapeutic target for high-risk neuroblastoma. *Mol Pharmacol* **70**:2108–2115.

Gentleman RC, Carey VJ, Huber W, Irizarry RA, and Dudoit S (2005) *Bioinformatics and Computational Biology Solutions Using R and Bioconductor,* Springer, New York.

Giacomini KM, Huang SM, Tweedie DJ, Benet LZ, Brouwer KL, Chu X, Dahlin A, Evers R, Fischer V, and Hillgren KM, et al.; International Transporter Consortium (2010) Membrane transporters in drug development. *Nat Rev Drug Discov* **9**:215–236.

Guitart X and Nestler EJ (1989) Identification of morphine- and cyclic AMP-regulated phosphoproteins (MARPPs) in the locus coeruleus and other regions of rat brain: regulation by acute and chronic morphine. *J Neurosci* **9**:4371–4387.

Hassan HE, Myers AL, Lee IJ, Chen H, Coop A, and Eddington ND (2010) Regulation of gene expression in brain tissues of rats repeatedly treated by the highly abused opioid agonist, oxycodone: microarray profiling and gene mapping analysis. *Drug Metab Dispos* **38**: 157–167.

Hassan HE, Myers AL, Lee IJ, Coop A, and Eddington ND (2007) Oxycodone induces overexpression of P-glycoprotein (ABCB1) and affects paclitaxel's tissue distribution in Sprague Dawley rats. *J Pharm Sci* **96**:2494–2506.

Hays LR (2004) A profile of OxyContin addiction. *J Addict Dis* **23**:1–9.

Heiskanen T, Olkkola KT, and Kalso E (1998) Effects of blocking CYP2D6 on the pharmacokinetics and pharmacodynamics of oxycodone. *Clin Pharmacol Ther* **64**:603–611.

Holtman JR, Jr and Wala EP (2006) Characterization of the antinociceptive effect of oxycodone in male and female rats. *Pharmacol Biochem Behav* **83**:100–108.

Homayoun H, Khavandgar S, Mehr SE, Namiranian K, and Dehpour AR (2003) The effects of FK506 on the development and expression of morphine tolerance and dependence in mice. *Behav Pharmacol* **14**:121–127.

Jover R, Ponsoda X, Gómez-Lechón J, and Castell JV (1993) Cocaine hepatotoxicity: two different toxicity mechanisms for phenobarbital-induced and non-induced rat hepatocytes. *Biochem Pharmacol* **46**:1967–1974.

Kalso E, Vainio A, Mattila MJ, Rosenberg PH, and Seppälä T (1990) Morphine and oxycodone in the management of cancer pain: plasma levels determined by chemical and radioreceptor assays. *Pharmacol Toxicol* **67**:322–328.

Kim RB (2002) Transporters and xenobiotic disposition. *Toxicology* **181-182**:291–297.

Kim WY and Benet LZ (2004) P-glycoprotein (P-gp/MDR1)-mediated efflux of sex-steroid hormones and modulation of P-gp expression in vitro. *Pharm Res* **21**:1284–1293.

Kloss MW, Cavagnaro J, Rosen GM, and Rauckman EJ (1982) Involvement of FAD-containing monooxygenase in cocaine-induced hepatotoxicity. *Toxicol Appl Pharmacol* **64**:88–93.

Laemmli UK (1970) Cleavage of structural proteins during the assembly of the head of bacteriophage T4. *Nature* **227**:680–685.

Lalovic B, Kharasch E, Hoffer C, Risler L, Liu-Chen LY, and Shen DD (2006) Pharmacokinetics and pharmacodynamics of oral oxycodone in healthy human subjects: role of circulating active metabolites. *Clin Pharmacol Ther* **79**:461–479.

LeCluyse EL, Alexandre E, Hamilton GA, Viollon-Abadie C, Coon DJ, Jolley S, and Richert L (2005) Isolation and culture of primary human hepatocytes. *Methods Mol Biol* **290**: 207–229.

Lee HK, Lewis LD, Tsongalis GJ, McMullin M, Schur BC, Wong SH, and Yeo KT (2006) Negative urine opioid screening caused by rifampin-mediated induction of oxycodone hepatic metabolism. *Clin Chim Acta* **367**:196–200.

Li H, Chen T, Cottrell J, and Wang H (2009) Nuclear translocation of adenoviral-enhanced yellow fluorescent protein-tagged-human constitutive androstane receptor (hCAR): a novel tool for screening hCAR activators in human primary hepatocytes. *Drug Metab Dispos* **37**: 1098–1106.

Li L, Hassan HE, Tolson AH, Ferguson SS, Eddington ND, and Wang H (2010) Differential activation of pregnane X receptor and constitutive androstane receptor by buprenorphine in primary human hepatocytes and HepG2 cells. *J Pharmacol Exp Ther* **335**:562–571.

Li L, Sinz MW, Zimmermann K, and Wang H (2012) An insulin-like growth factor 1 receptor inhibitor induces CYP3A4 expression through a pregnane X receptor-independent, non-canonical constitutive androstane receptor-related mechanism. *J Pharmacol Exp Ther* **340**: 688–697.

Lin JH (2003) Drug-drug interaction mediated by inhibition and induction of P-glycoprotein. *Adv Drug Deliv Rev* **55**:53–81.

McClung CA, Nestler EJ, and Zachariou V (2005) Regulation of gene expression by chronic morphine and morphine withdrawal in the locus ceruleus and ventral tegmental area. *J Neurosci* **25**:6005–6015.

Myers AL, Hassan HE, Lee IJ, and Eddington ND (2010) Repeated administration of oxycodone modifies the gene expression of several drug metabolising enzymes in the hepatic tissue of male Sprague-Dawley rats, including glutathione S-transferase A-5 (rGSTA5) and CYP3A2. *J Pharm Pharmacol* **62**:189–196.

Nakazawa Y, Okura T, Shimomura K, Terasaki T, and Deguchi Y (2010) Drug-drug interaction between oxycodone and adjuvant analgesics in blood-brain barrier transport and antinociceptive effect. *J Pharm Sci* **99**:467–474.

Nielsen CK, Ross FB, and Smith MT (2000) Incomplete, asymmetric, and route-dependent cross-tolerance between oxycodone and morphine in the Dark Agouti rat. *J Pharmacol Exp Ther* **295**: 91–99.

Nieminen TH, Hagelberg NM, Saari TI, Neuvonen M, Laine K, Neuvonen PJ, and Olkkola KT (2010) St John's wort greatly reduces the concentrations of oral oxycodone. *Eur J Pain* **14**: 854–859.

Nieminen TH, Hagelberg NM, Saari TI, Pertovaara A, Neuvonen M, Laine K, Neuvonen PJ, and Olkkola KT (2009) Rifampin greatly reduces the plasma concentrations of intravenous and oral oxycodone. *Anesthesiology* **110**:1371–1378.

Pöyhiä R and Kalso EA (1992) Antinociceptive effects and central nervous system depression caused by oxycodone and morphine in rats. *Pharmacol Toxicol* **70**:125–130.

Shippy R, Sendera TJ, Lockner R, Palaniappan C, Kaysser-Kranich T, Watts G, and Alsobrook J (2004) Performance evaluation of commercial short-oligonucleotide microarrays and the impact of noise in making cross-platform correlations. *BMC Genomics* **5**:61.

Tirona RG and Kim RB (2005) Nuclear receptors and drug disposition gene regulation. *J Pharm Sci* **94**:1169–1186.

Tolson AH, Li H, Eddington ND, and Wang H (2009) Methadone induces the expression of hepatic drug-metabolizing enzymes through the activation of pregnane X receptor and constitutive androstane receptor. *Drug Metab Dispos* **37**:1887–1894.

Tono T, Iwazawa T, Matsui S, Yano H, Kimura Y, Kanoh T, Ohnishi T, Nakano Y, Okamura J, and Monden T (2004) Hepatic arterial infusion of paclitaxel for liver metastasis from gastric cancer. *Cancer Invest* **22**:550–554.

van der Hoeven TA and Coon MJ (1974) Preparation and properties of partially purified cytochrome P-450 and reduced nicotinamide adenine dinucleotide phosphate-cytochrome P-450 reductase from rabbit liver microsomes. *J Biol Chem* **249**:6302–6310.

Vanwert AL, Bailey RM, and Sweet DH (2007) Organic anion transporter 3 (Oat3/Slc22a8) knockout mice exhibit altered clearance and distribution of penicillin G. *Am J Physiol Renal Physiol* **293**:F1332–F1341.

VanWert AL and Sweet DH (2008) Impaired clearance of methotrexate in organic anion transporter 3 (Slc22a8) knockout mice: a gender specific impact of reduced folates. *Pharm Res* **25**: 453–462.

Wang H, Faucette SR, Gilbert D, Jolley SL, Sueyoshi T, Negishi M, and LeCluyse EL (2003) Glucocorticoid receptor enhancement of pregnane X receptor-mediated CYP2B6 regulation in primary human hepatocytes. *Drug Metab Dispos* **31**:620–630.

Waxman DJ (1984) Rat hepatic cytochrome P-450 isoenzyme 2c. Identification as a male-specific, developmentally induced steroid 16 alpha-hydroxylase and comparison to a female-specific cytochrome P-450 isoenzyme. *J Biol Chem* **259**:15481–15490.

Weinstein SH and Gaylord JC (1979) Determination of oxycodone in plasma and identification of a major metabolite. *J Pharm Sci* **68**:527–528.

Wu Z, Irizarry RA, Gentleman R, Martine-Murillo F, and Spencer F (2004) A model-based background adjustment for oligonucleotide expression arrays. *J Am Stat Assoc* **99**: 909–917.

Yue J, Khokhar J, Miksys S, and Tyndale RF (2009) Differential induction of ethanol-metabolizing CYP2E1 and nicotine-metabolizing CYP2B1/2 in rat liver by chronic nicotine treatment and voluntary ethanol intake. *Eur J Pharmacol* **609**:88–95.

Zhu Z, Kim S, Chen T, Lin JH, Bell A, Bryson J, Dubaquie Y, Yan N, Yanchunas J, and Xie D, et al. (2004) Correlation of high-throughput pregnane X receptor (PXR) transactivation and binding assays. *J Biomol Screen* **9**:533–540.

Zhu Z, Puglisi J, Connors D, Stewart J, Herbst J, Marino A, Sinz M, O'Connell J, Banks M, and Dickinson K, et al. (2007) Use of cryopreserved transiently transfected cells in high-throughput pregnane X receptor transactivation assay. *J Biomol Screen* **12**:248–254.

Address correspondence to: Dr. Natalie D. Eddington, FAAPS, FCP, University of Maryland, School of Pharmacy, 20 N. Pine Street, N307, Baltimore, MD 21201. E-mail: neddingt@rx.umaryland.edu